Dual-Readout Calorimetry for High-Quality Energy Measurements

Progress Report

Presented by:

Dr. Gabriella Gaudio, Dr. John Hauptman and Dr. Richard Wigmans[1]

on behalf of the RD52 (DREAM) Collaboration

(Cagliari - Cosenza - Iowa State - Lisbon - Pavia - Pisa - Roma I - Texas Tech)

CERN-SPSC-2014-010 / SPSC-SR-135
24/03/2014

8 April 2014

[1]Contact person. Tel. [806] 742 3779, FAX [806] 742 1182, E-mail: wigmans@ttu.edu

1 Introduction

On August 31, 2011, the CERN Research Board decided to accept the DREAM Collaboration's detector R&D proposal [1] and included it as project RD52 in its official scientific program. This document constitutes the third RD52 progress report. In this report, we describe our activities since the last time we reported to the SPS Committee (April 9, 2013 [2]), as well as our future plans.

Since the SPS was shut down during this reporting period, no new experimental data have been collected. Instead, we have used the past year to analyze all the data collect in December 2012, just before the shutdown, and have written papers in which these analyses are described [3, 4, 5, 6]. We have also carried out an elaborate program of Monte Carlo simulations of the performance of the unusual calorimeters that are the topic of our studies. A paper on these results [7] has also been submitted for publication.

We are in the process of preparing for a new round of experimental data taking. New copper based calorimeter modules are under construction in Iowa. We are planning to build a calorimeter consisting of 4×4 copper based modules, containing 64 towers and thus producing 128 signals for each event. Proper testing of this instrument (which involves calibrating 128 photomultiplier tubes with an electron beam) will require an uninterrupted test beam period of at least two weeks. Since that seems to be not in the realm of possibilities for the 2014 SPS campaign, we will dedicate the week allocated at the end of the year to additional studies of the electromagnetic performance, which are inspired by the Monte Carlo predictions.

In the past year, the latest RD52 results have been presented at the EPS Conference in Stockholm (Sweden), the IEEE Nuclear Science Symposium in Seoul (Korea) and the 13th Topical Seminar on Innovative Particle and Radiation Detection (Siena, Italy). The talks, as well as all publications in the context of this project, can be found at the RD52 website:
http://highenergy.phys.ttu.edu/dream/results/talks/talks.html

Details about our various past, current and planned activities are given in the next sections.

2 New experimental results

In the past year, a lot of effort has gone into analyses of the experimental data taken in our most recent test beam campaigns. This work has resulted in the following publications:

1. *New Results from the RD52 (DREAM) Project*
   R. Wigmans, Nucl. Instr. and Meth. **A718** (2013) 43 - 47.

2. *The dual-readout approach to calorimetry*
   R. Wigmans, Nucl. Instr. and Meth. **A732** (2013) 475 - 479.

3. *Particle identification in the longitudinally unsegmented RD52 calorimeter*
   N. Akchurin *et al.*, Nucl. Instr. and Meth. **A735** (2014) 120 - 129.

4. *The electromagnetic performance of the RD52 fiber calorimeter*
   N. Akchurin *et al.*, Nucl. Instr. and Meth. **A735** (2014) 130 - 144.

The first two papers concern contributions to the Proceedings of the Instrumentation conferences in Elba (May 2012) and Vienna (February 2013). Papers 3 and 4 contain the results of the beam tests carried out in December 2012. One unique aspect of the fiber calorimeters we are building is the fact that they are longitudinally *unsegmented*. Traditionally, the calorimeter systems in high-energy physics experiments are separated into (at least) two sections: the electromagnetic (em) and the hadronic section. This arrangement offers a certain number of advantages, especially for the identification of electrons and photons, which deposit all their energy in the em section and can thus be identified as such based on this characteristic.

Yet, there are also substantial disadvantages, especially for what concerns the detection of hadrons and hadron jets. Hadrons deposit typically some fraction of their energy in each section, with very large event-to-event fluctuations in the energy sharing between the sections. The response, *i.e.* the average signal per GeV deposited energy, is typically considerably smaller for hadrons than for electrons of the same energy. This is a consequence of the fact that in hadron showers a considerable fraction of the energy is used to break up atomic nuclei, and this energy does not contribute to the calorimeter signals. This energy fraction is, on average, dependent on the energy of the showering particles, and varies strongly from event to event. These characteristics lead to problems in determining the energy of the showering hadrons and jets, since it is not obvious how to convert the measured signals into deposited energy.

The RD52 Collaboration has demonstrated that these *jet energy scale* problems can be avoided in dual-readout fiber calorimeters [8, 9, 10]. In these devices, the precision with which the energy of single hadrons and jets can be measured is greatly improved by simultaneous measurements of the deposited energy and the fraction of that energy carried by relativistic charged shower particles, which are predominantly electrons and positrons. These measurements make it possible to measure the em component of these showers ($f_{\rm em}$) event by event. In this way, the effects of fluctuations in $f_{\rm em}$, which tend to dominate the hadronic energy resolution of calorimeters, are eliminated, and the response can be trivially equalized to that of purely em showers (for which $f_{\rm em} = 1$), such as the ones generated by electrons.

The question how well electrons and photons can be identified in such a longitudinally unsegmented calorimeter is the topic of paper 3 [4]. We have developed four different methods that make this possible. These methods are based on

1. The lateral shower profile
2. A comparison of the scintillation and Čerenkov signals
3. The time structure of the events

The last characteristic offers possibilities to distinguish particles developing em and hadronic showers by means of the starting time of the pulse and/or the pulse width. Figure 1 illustrates how well these different methods work in practice. It turns out that by combining different e/π separation methods, important improvements can be achieved in the capability of our longitudinally unsegmented calorimeter to identify electrons, with minimal contamination of misidentified particles. For example, as illustrated in Figures 1a,c, 99.1% of electrons and less than 0.5% of the pions passed the combination of the cuts $f_{\rm cut} > 0.70$ (method a) and $t_s({\rm cut}) > 28.0$ ns (method c). This illustrates that these two types of cuts are completely uncorrelated, which

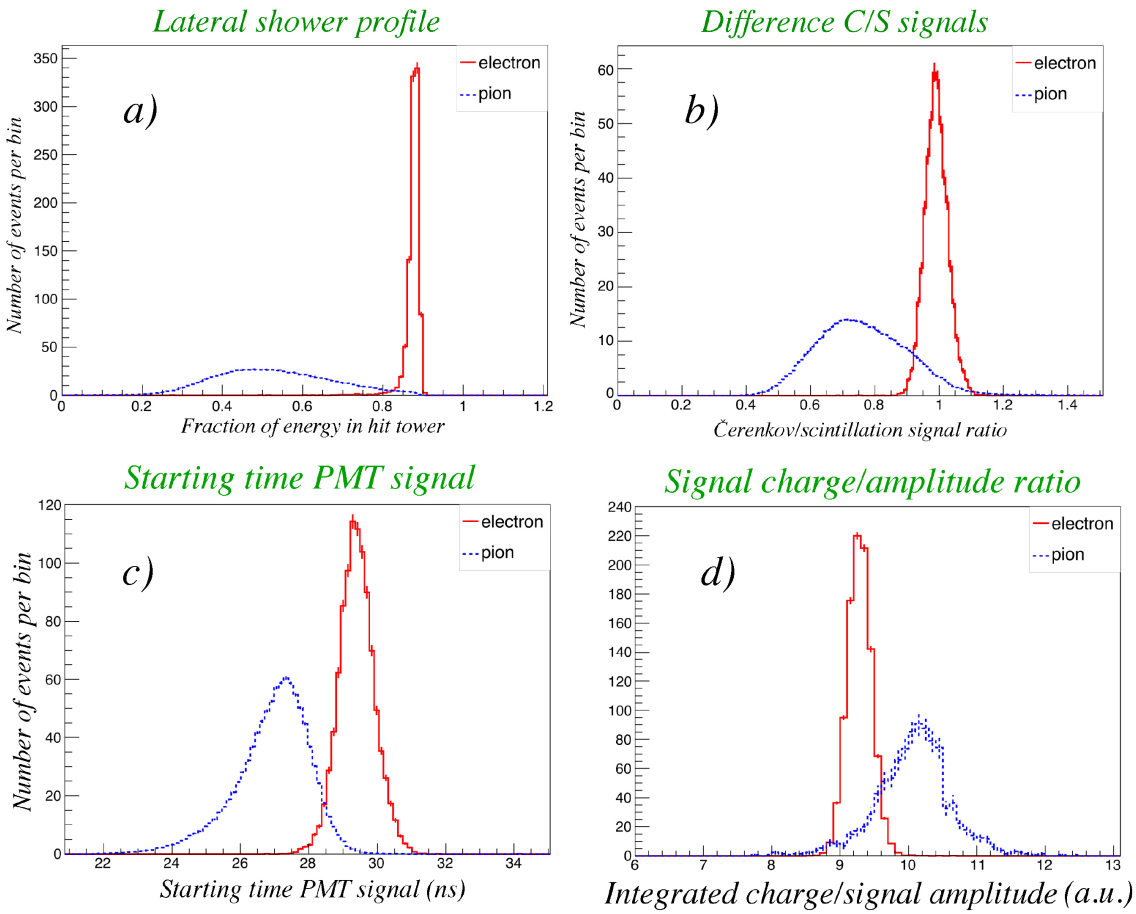

Figure 1: Electron/hadron separation in the longitudinally unsegmented RD52 fiber calorimeter. Shown are the measured distributions for electrons and pions in terms of the lateral shower profile (a), the ratio of the Čerenkov and scintillation signals (b), the starting time of the PMT signals (c) and the ratio of the integrated charge and the amplitude of the signals (d).

is no surprise since the first cut discriminates on the basis of the lateral shower shape, and the second cut on the depth at which the shower started. Using the Čerenkov/scintillation characteristics, a cut $(C/S)_{\rm cut} > 0.85$ (method b) further improved the purity of the electron sample. The remaining mis-identified pions are predominantly particles that interact close to the front face of the calorimeter and transfer a large fraction of their energy to one or several π^0s. Charge exchange reactions ($\pi^- + p \rightarrow \pi^0 + n$) fall into this category.

Of course, there are in principle many different combinations of cuts that achieve approximately the same results as quoted above. A multivariate neural network analysis showed that the best e/π separation achievable with the three variables used for the 60 GeV beams was 99.8% electron identification with 0.2% pion misidentification (for $MLP > 0.17$, see Figure 2). Further improvements may be expected by including the full time structure information of the pulses, especially if the upstream ends of the fibers are made reflective [11].

The fact that no longitudinal segmentation is applied leads to an important reduction in the channel count, in comparison, for example, with calorimeter systems based on Particle Flow

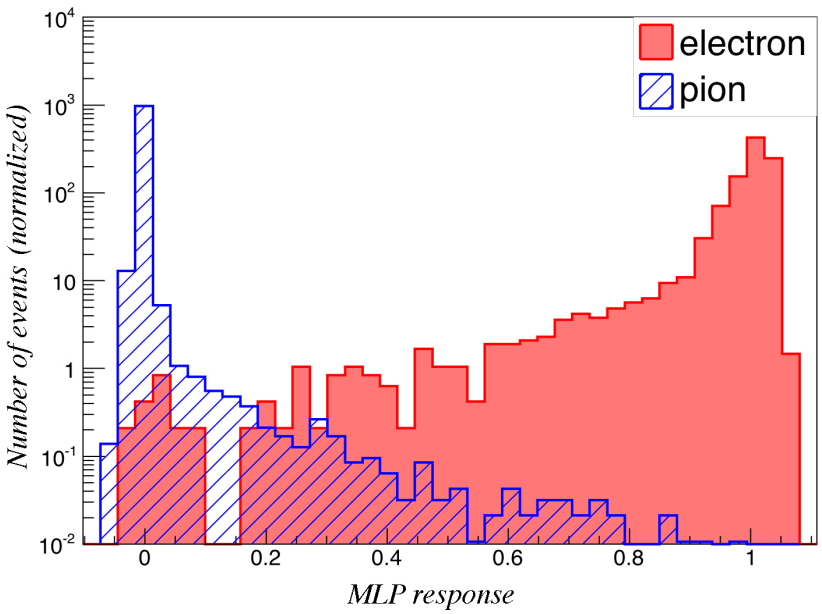

Figure 2: Results from the multivariate analysis of the electron/pion separability at 60 GeV, which made simultaneous use of the lateral shower profile, the Čerenkov/scintillation signal ratio and the starting time of the PMT signals as the event characteristics that allowed distinguishing electrons from pions. The multi-layer perception (MLP) response indicates that 99.8% of all electrons could be identified with a combination of criteria that rules out 99.8% of all pions as electron candidates.

Analysis [12]. On the other hand, the fiber readout does make it possible to make a much finer *lateral* granularity than in other types of calorimeters. This may create the possibility to recognize, identify and measure the properties of electrons in a very dense particle environment, *e.g.* inside multiparticle jets. This is because electron showers have a very pronounced collimated core, with a width of only a few mm, as illustrated in Figure 3, which shows the result of a measurement performed with the RD52 fiber calorimeter.

The analysis of the measured em shower profile was carried out in the context of the fourth paper listed at the beginning of this section [5]. The central core represents the early, extremely collimated portion of the shower development, in which the electrons and positrons that produce the signal are travelling very close to the shower axis. It is interesting, and consistent with information on the response function, that this core seems to be less pronounced when measured for the Čerenkov signals.

Other topics studied in the context of this paper included the signal linearity, the angular dependence of the response ratio of the two types of signals, and of course the em energy resolution. A major difference with the original DREAM fiber module concerns the fact that each fiber is now individually embedded in the absorber structure, whereas the fibers were bunched together in groups of seven in the DREAM module. The fiber density has also been increased by about a factor of two with respect to the original DREAM module. As a result, the contribution of sampling fluctuations to the energy resolution[1] has been reduced by a factor 2.2.

[1]This contribution scales like $\sqrt{d/f_{\rm samp}}$, where d represents the fiber thickness and $f_{\rm samp}$ the sampling fraction [13].

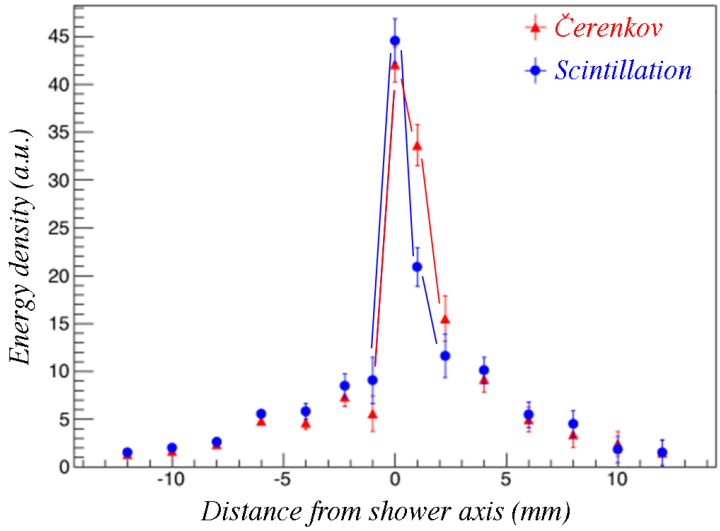

Figure 3: The lateral profile of 100 GeV electron showers developing in the RD52 calorimeter, measured separately with the scintillation and the Čerenkov signals [5].

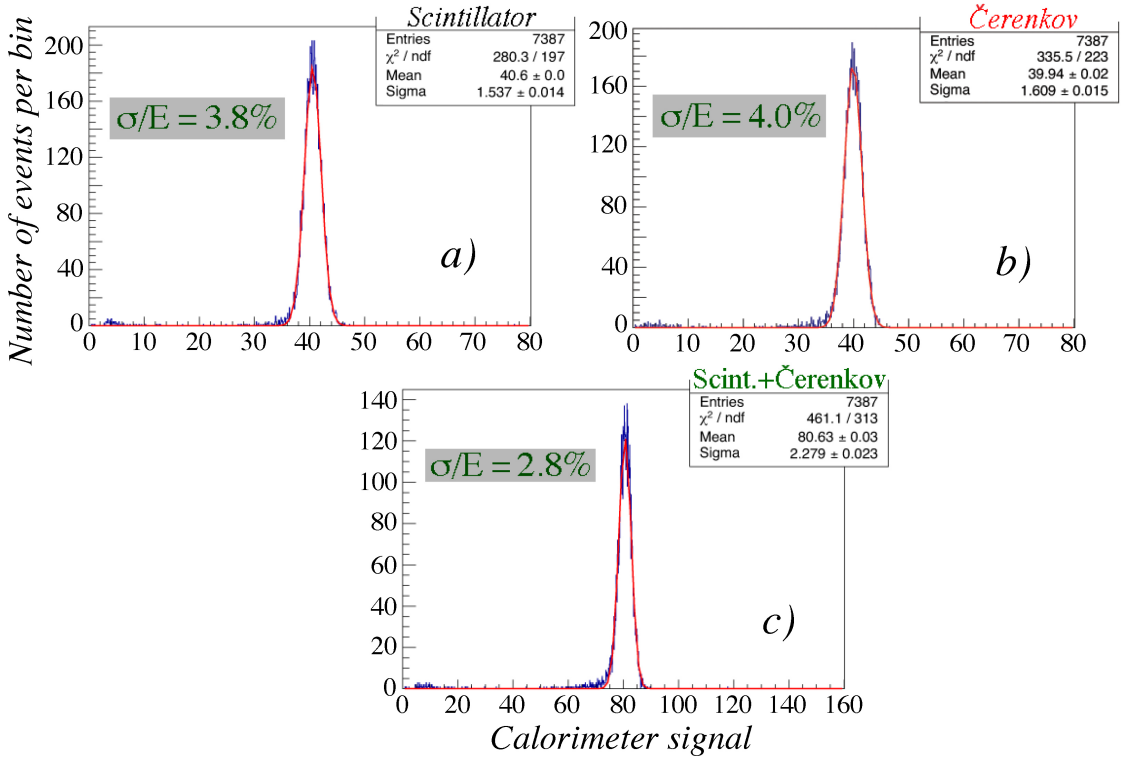

Figure 4: Signal distributions for 40 GeV electrons in the copper-fiber calorimeter. Shown are the distributions measured with the scintillating fibers (a), the Čerenkov fibres (b) and the sum of all fibers (c). The angle of incidence (ϕ, θ) of the electrons was (1.5°, 1.0°).

An additional advantage of the new fiber pattern is the fact that the scintillation and Čerenkov readout represent completely independent sampling structures. Therefore, by combining the signals from the two types of fibers, a significant improvement in the energy resolution is obtained. This was not the case for DREAM, where the two types of fibers essentially sampled the showers in the same way.

The changes in the structure of the fiber module did indeed pay off in the form of a substantially improved em energy resolution. Figure 4 shows the response functions for 40 GeV electrons in the copper based RD52 fiber calorimeter. The energy resolutions measured with the scintillating (fig. 4a) and Čerenkov (fig. 4b) fibers are almost the same, while the resolution measured with the sum of all fibers (fig. 4c) is almost a factor of $\sqrt{2}$ better, at 2.8%, an improvemment by a factor of ~ 2.5 with respect to the original DREAM calorimeter. As a matter of fact, the improvement would have been even larger if the measurements had been carried out with electrons at the same angle of incidence with respect to the fibers. This angle is important because there is in this type of calorimeter a systematic response difference between particles entering the calorimeter in a fiber or in the absorber material between fibers. This difference, which is caused by the extremely collimated core of the em showers (fig. 3), vanishes as the angle of incidence increases and is barely noticeable for angles larger than $\sim 3^\circ$. The greatly reduced distance between neighboring fibers makes the response (and thus the energy resolution) much less sensitive to the impact point of the electrons in the RD52 calorimeter, compared to DREAM. Yet, the effect is not completely absent, at least for the scintillation response function. This may be concluded from the energy dependence of the energy resolution (Figure 5). A position dependent response leads to an energy independent term in the energy resolution. In Figure 5, the energy resolution is plotted on a scale linear in $-E^{-1/2}$, so that a resolution that scales with $1/\sqrt{E}$ is described by a straight line through the bottom right corner ($E = \infty$) in such a plot. The resolution measured with the Čerenkov fibers is well described by such a line,

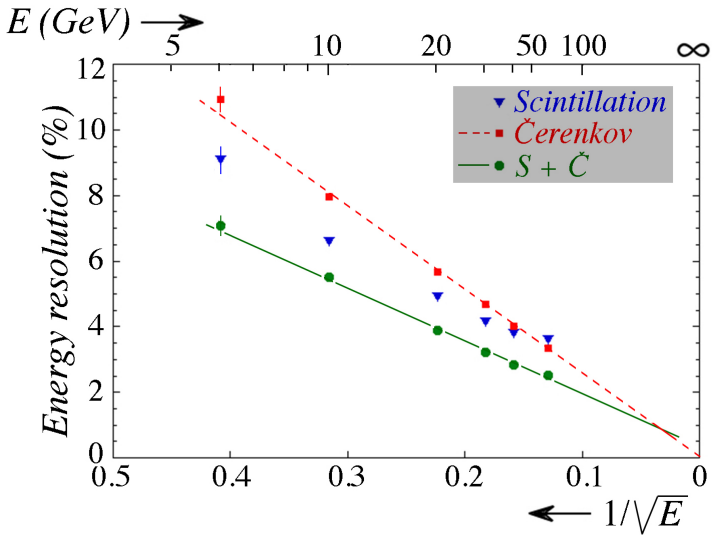

Figure 5: The energy resolution for electrons in the copper-fiber module, as a function of the beam energy. Shown are the results for the two types of fibers, and for the combined signals. The angle of incidence (ϕ, θ) of the electrons was (1.5°, 1.0°).

but the scintillation resolution clearly shows a deviation that suggests an energy independent contribution of $\sim 2\%$. As a result, at high energy the measured resolution is even better for the Čerenkov signals than for the scintillation ones, despite the fact that the stochastic fluctuations (light yield!) are considerably larger.

The reason why the impact point dependence of the response function is absent for the Čerenkov signals is the fact that the very collimated, narrow core that characterizes the early phase of em showers does *not* contribute to the Čerenkov signals, since the Čerenkov light generated in this phase falls outside the numerical aperture of the fibers [14].

The combined signals scale reasonably well with $1/\sqrt{E}$. A fit to the experimental points yielded a scaling term of $13.9\%/\sqrt{E}$ and an energy independent term of $\sim 0.5\%$. The contribution of sampling fluctuations to the scaling term was found to be $8.9\%/\sqrt{E}$, with fluctuations in photoelectron statistics being responsible for the difference. The light yield in the different towers was measured to vary between 20 - 40 photoelectrons per GeV deposited energy for the Čerenkov signals and 100 - 200 photoelectrons per GeV for the (yellow-filtered) scintillation signals.

3 Monte Carlo simulations

Inspired by the wealth of new results obtained in the last few years, we embarked in 2013 on an elaborate program of Monte Carlo simulations of our, in many ways, very unusual calorimeters. The purpose of these simulations, based on GEANT4, was twofold:

1. To test the (limits of the) validity of such simulations with experimental data already obtained. In particular, we were interested in the dependence of the response function and the energy resolution on parameters such as the particle's energy and its angle of incidence.

2. To predict the effects on the performance for certain modifications of the detectors, for example a larger instrumented mass, an increased light yield, or a different choice of absorber medium.

The results of this work, which consumed a few thousand CPU hours on the computer systems at our disposal, are described in a new paper that was recently submitted for publication:

- *Lessons from Monte Carlo simulations of the performance of a dual-readout fiber calorimeter*, N. Akchurin *et al.*, submitted to Nucl. Instr. and Meth. in Phys. Res.

In the following, a selection of the results is shown.

3.1 The electromagnetic performance

The differences between the response functions of the two types of fibers, discussed in Section 2, was confirmed by the Monte Carlo simulations. Figure 6 shows that for angles of incidence $\lesssim 2^\circ$ the response function for the Čerenkov signals is much better described by a Gaussian shape than the response function for the scintillation signals. This is evident both from the χ^2

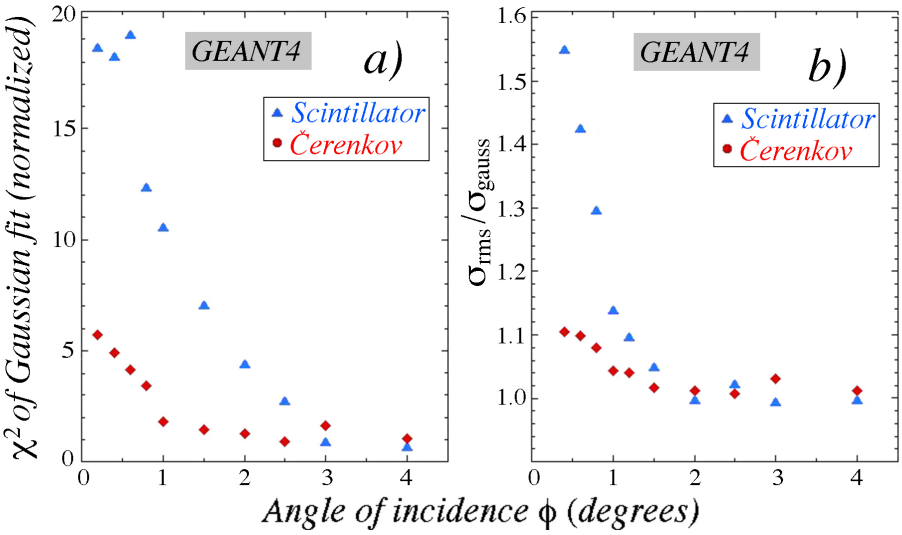

Figure 6: The χ^2 of a Gaussian fit to the response function (a) and the ratio of the rms width and the σ of a Gaussian fit (b) as a function of the angle of incidence ϕ of the 40 GeV electrons. The tilt angle θ was chosen to be 1° in all these GEANT4 simulations. Results are given separately for the scintillation and Čerenkov signals in the lead structure.

values of the Gaussian fits (fig. 6a) and from the ratio of the *rms* and the Gaussian widths of the signal distributions (fig. 6b). This feature has also repercussions for the em energy resolution. At 40 GeV, the resolution is actually better for the Čerenkov signals than for the scintillation ones when the electrons enter the calorimeter at angles $< 2^\circ$ (Figure 7).

Figures 6 and 7 are both for calorimeters with lead as absorber material. Interestingly, we found that the Monte Carlo simulations predicted that a copper based calorimeter should be

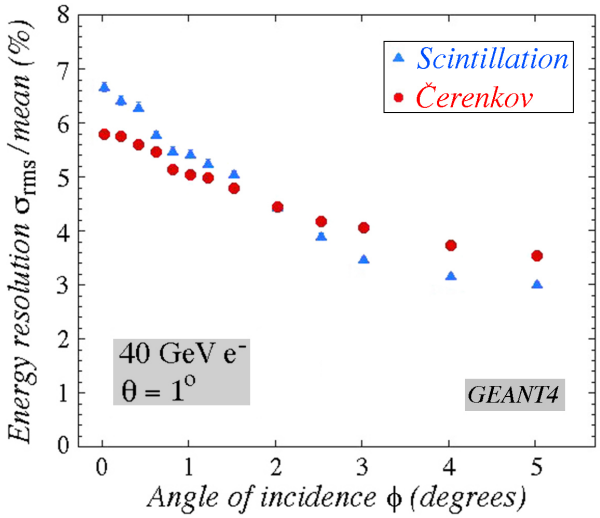

Figure 7: The dependence of the energy resolution on the angle of incidence ϕ. Results for 40 GeV electrons in the lead calorimeter structure. The tilt angle θ was 1° in these simulations.

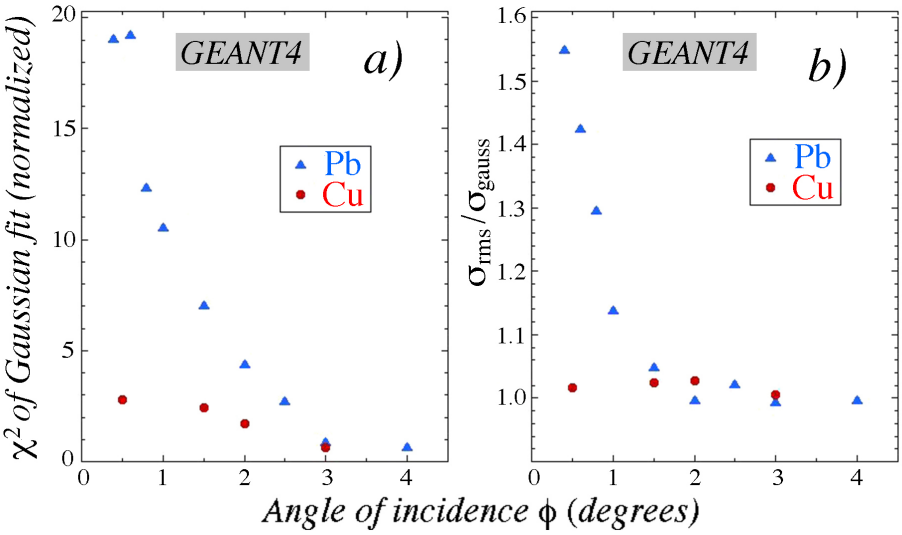

Figure 8: The χ^2 of a Gaussian fit to the response function (a) and the ratio of the rms width and the σ of a Gaussian fit (b) as a function of the angle of incidence ϕ of the 40 GeV electrons. The tilt angle θ was chosen to be 1° in all simulations. Results are given separately for these GEANT4 simulations of em shower development in the lead and copper/scintillating-fiber structures.

less sensitive to these impact point dependent effects. This is illustrated in Figure 8, which compares the angular dependence of the quality of a Gaussian fit to the scintillation response functions for 40 GeV electrons in lead and copper based RD52 fiber calorimeter structures. We have learned from these simulations that the orgin of this difference is the fact that the radiation length of copper is almost three times larger than for lead, while the Moliere radii (which govern the radial shower development) are about the same. This means that the early, extremely collimated shower extends much deeper into the copper structure than into the lead one, and is therefore much more likely to be sampled by several different fibers at a given, very small angle of incidence.

We also used these simulations to estimate the improvement in the em energy resolution that might be expected as a result of further increasing the Čerenkov light yield. With new photocathode materials that are now becoming available on the market, it is estimated that the quantum efficiency of our PMTs could be increased by a factor of 2 - 3. Additional gains may be obtained by aluminizing the upstream ends of the Čerenkov fibers.

Figure 9 shows how an increase of the Čerenkov light yield would improve the em energy resolution of the Čerenkov signals and the combined resolution from all fibers. The improvement is significant, especially at low energies, albeit not spectacular.

Even though many features of the em performance of the RD52 calorimeters, both for electron and muon detection, were accurately described by these GEANT4 simulations, there were also some areas in which the Monte Carlo predictions were not confirmed by experimental data, or plainly wrong. We would like to investigate these issues further and come back to this in Section 4, where we discuss our plans for beam tests in 2014.

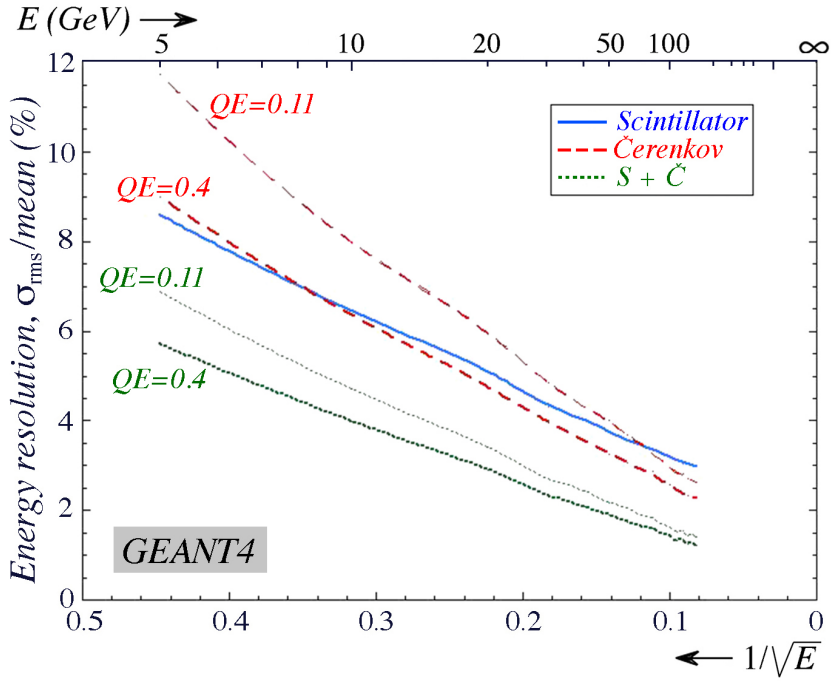

Figure 9: The predicted effect of an increase in the Čerenkov light yield on the em energy resolution of the copper calorimeter. See text for details.

3.2 The hadronic performance

The available experimental hadron data with which the Monte Carlo predictions could be confronted were much more limited than the em ones. Because of the absence of a sufficiently large calorimeter, we limited ourselves for copper to the data taken with the original DREAM calorimeter. Figure 10 shows the response functions of the scintillating and the Čerenkov fibers for 100 GeV π^- in this dual-readout copper-fiber calorimeter. The experimental data were published in [8], the simulated results in [7]. GEANT4 offers a wide variety of packages describing the hadronic shower development. These particular response functions were obtained with the FTFP_BERT package, which is the standard used by the ATLAS and CMS collaborations. It turns out that the Čerenkov response function is well described by the simulations. On the other hand, the scintillation distribution is more narrow, less asymmetric and peaks at a lower value than for the experimental data. We tried several other hadronic packages, but these did not fundamentally change these findings. We also found that the hadronic signal non-linearity, which is typical for every non-compensating calorimeter, was much better described for the Čerenkov signals than for the scintillation ones.

From additional analyses, we established that the non-relativistic component of the shower development, which is completely dominated by processes at the nuclear level, is rather poorly described by GEANT4. Both the average size of this component, as well as its event-to-event fluctuations, are at variance with the experimental data. This non-relativistic shower component only plays a role for the scintillation signals, *not* for the Čerenkov ones.

Yet, some aspects of hadronic shower development that are important for the dual-readout

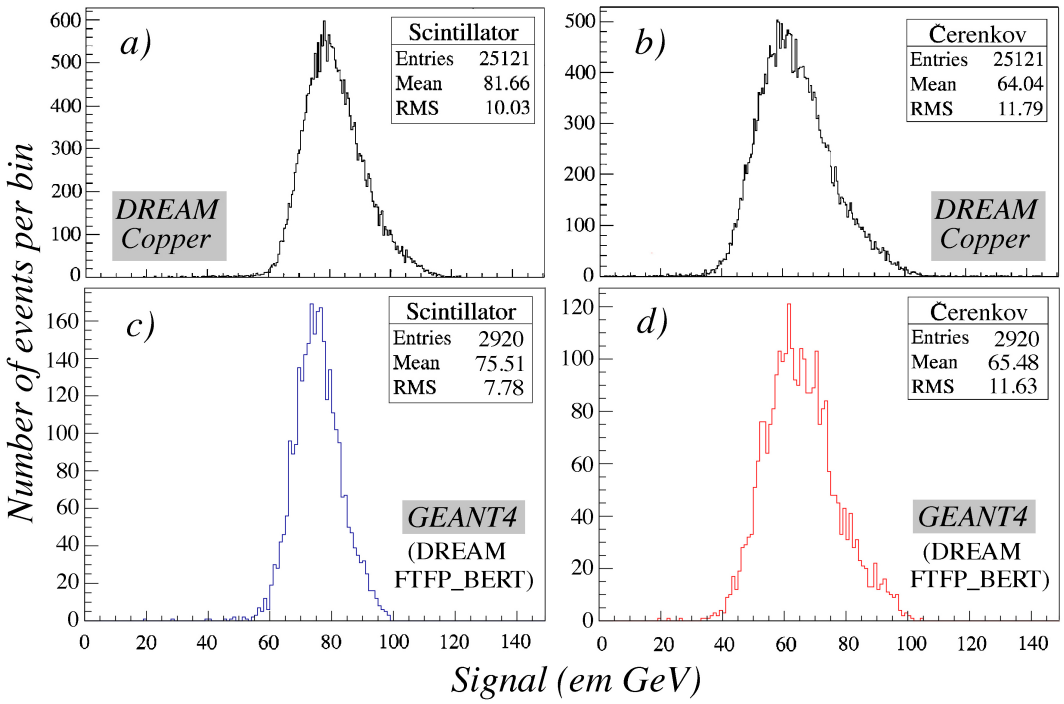

Figure 10: The response functions for 100 GeV pions in the copper based DREAM calorimeter. Shown are the experimental data measured for the scintillation (a) and Čerenkov (b) signals [8], as well as the simulated response functions for these two types of signals in the DREAM geometry (c, d), using the FTFP_BERT package.

application are in good agreement with the experimental data. As examples, we mention the shape of the Čerenkov response function and the radial shower profiles. Attempts to use the dual-readout technique on simulated shower data reasonably reproduced some of the essential characteristics and advantages of this method: A Gaussian response function, hadronic signal linearity and improved hadronic energy resolution. The fact that the reconstructed beam energy is systematically too low may be ascribed to the problems with the non-relativistic shower component mentioned above.

An important reason for performing these very time consuming simulations was to see if and to what extent the hadronic performance would improve as the detector size is increased. Figure 11a shows the resolution of a copper based RD52 calorimeter for 100 GeV π^- as a function of the size of the calorimeter. We used a structure consisting of 9 (3×3), 25 (5×5) and 49 (7×7) modules of the type currently built by our collaboration for these simulations. According to the simulations, the resolution (achieved with the dual-readout method) would improve from 7.3% (3×3) to 5.2% (5×5) to 4.6% (7×7). The response function for the latter case is shown in figure 11b. Figure 12 summarizes the situation concerning the hadronic energy resolution, for single pions. It shows experimental data obtained with the DREAM [8] and RD52_Pb [6] calorimeters, as well as the record setting results published by SPACAL [15]. Also shown are the GEANT4 predictions for a 3×3 and 7×7 module RD52_Cu calorimeter [7].

We believe that the predicted improvement in the performance resulting from an increased detector size is realistic. The resolution of the instruments tested so far was clearly dominated

Improvement in resolution when calorimeter enlarged (GEANT4)

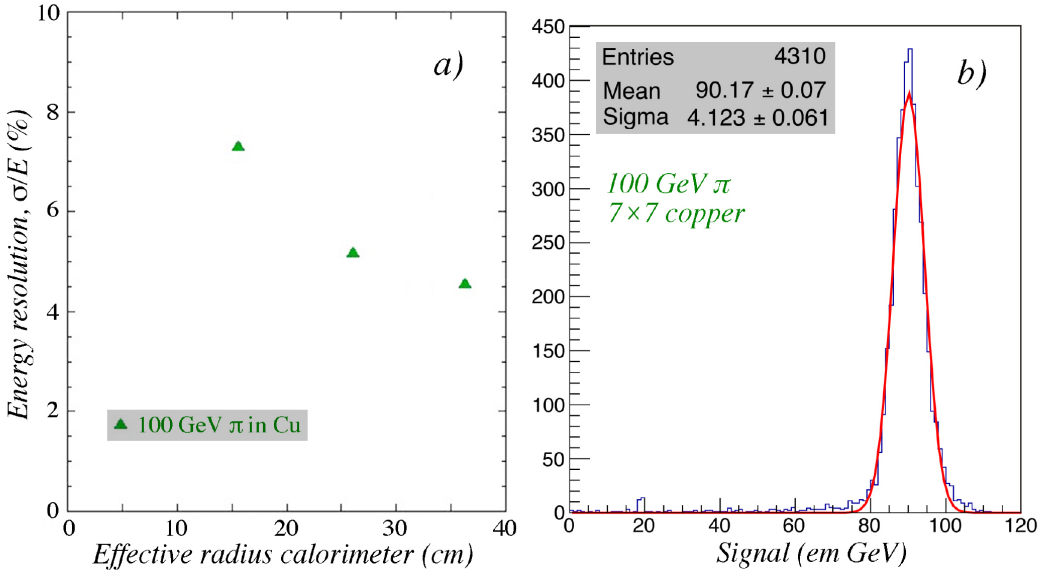

Figure 11: The energy resolution for 100 GeV pions in a dual-readout fiber calorimeter based on copper absorber, as a function of the radial size of the calorimeter (a). The reconstructed energy distribution for 100 GeV pions in a 7×7 module dual-readout copper-fiber calorimeter (b). Results of GEANT4 Monte Carlo simulations.

by leakage fluctuations. An increase in the detector volume would reduce the effects of this, in which case resolutions of a few percent seem to be feasible, and would bring the hadronic performance of the RD52 at the same level as that of the compensating SPACAL and ZEUS calorimeters.

It should be emphasized that the results shown in Figures 11 and 12 are for *single hadrons*. Therefore, energy independent contributions from light attenuation in the fibers are by no means negligible. If the effective nuclear interaction length of the calorimeter is 25 cm, then an attenuation length of 10 m leads to an energy independent term in the resolution of 2.5%. The SPACAL data, which were corrected event-by-event for these effects, illustrate this point (Figure 12).

When detecting jets, the effects of light attenuation are considerably smaller, since the jet consists of a number of particles, each of which develops its own shower. Moreover, the γ component (from π^0 decay) is exempt from these attenuation effects altogether. However, there is an important reason why the jet resolution of copper based dual-readout fiber calorimeters may be expected to be much better than that of the high-Z compensating calorimeters [16]. A sizable component of the jet consists of soft hadrons, which range out rather than developing showers. The response of calorimeters such as ZEUS to these particles is considerably larger than the response to the showering γs and high-energy hadrons. The scale for the difference between these responses is set by the e/mip value, which was measured to be 0.62 in ZEUS and 0.72 in SPACAL. The advantage of an absorber material with much lower Z is an e/mip value that is much closer to 1 (the value at which point this effect ceases to play a role). For our copper based dual-readout fiber calorimeter, an e/mip value of 0.84 was found.

The possibility to measure jets with superior resolution compared to previously built high-Z

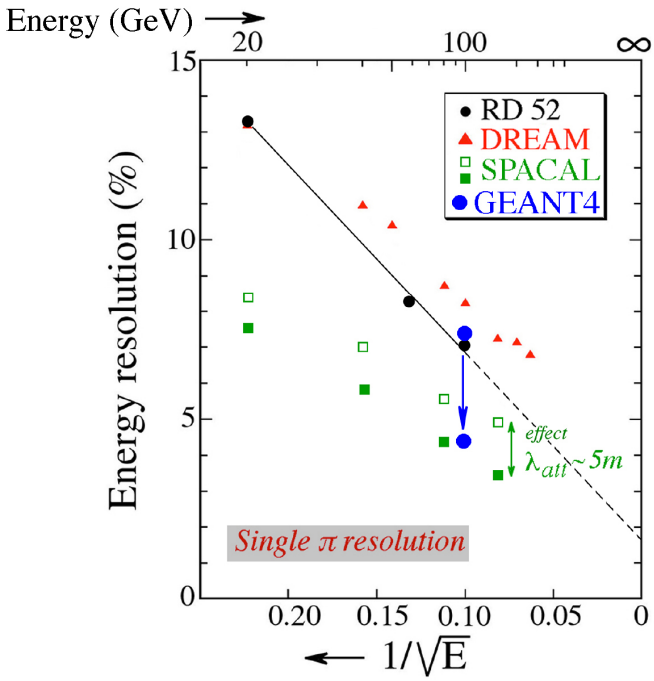

Figure 12: The energy resolution for single pions measured with the dual-readout DREAM [8] and RD52 [6] calorimeters. For comparison, the resolutions measured with the high-resolution SPACAL calorimeter are shown as well (before and after corrections for the effects of light attenuation in the fibers were applied) [15]. Also shown are the results of GEANT4 simulations for the current and full-size RD52 copper-fiber calorimeter [7]. See text for details.

compensating calorimeters was one of the main reasons why we embarked on the dual-readout project.

4 Future plans

4.1 Plans for 2014

In 2014, the availability of the SPS will be very limited. In the provisional schedule recently distributed by the SPS coordinator, RD52 has been allocated 7 days of beam time in H8. This is not enough for a serious test program of the new hadron calorimeter, which in any case has to start with calibrating 128 individual PMTs, by means of an electron beam. Even in the most optimistic scnenario, this calibration itself would require 3 full days.

Therefore, we will concentrate in the allocated week on our remaining test program with em showers and muons. The test program with jets and hadrons will have to wait until 2015, when hopefully a 2-week beam period can be scheduled.

The program we would like to carry out in 2014 is partly inspired by the Monte Carlo results discussed in subsection 3.1. It contains the following components:

- An angular scan of the lead based calorimeter, in small steps with electrons of one energy, *e.g.* 40 GeV. This would allow us to verify the predictions concerning the differences

between the lineshapes of the two types of signals (Figure 6) as a function of the angle of incidence. This scan would also allow us to check the predicted angular dependence of the em energy resolution (Figure 7).

- This angular scan should be repeated for the copper based calorimeter, so that the predictions concerning the differences between the two absorber materials can be verified (Figure 8).

- These angular scans should be repeated for electrons at a higher energy, *e.g.* 100 GeV, at which the effects of the impact point dependence on the energy resolution should be much larger. This would make it possible to measure the energy independent contribution to the em energy resolution as a function of the angle of incidence, both for copper and lead absorber. This information will be very valuable for the design of a future calorimeter for an experiment in particle physics, since this design can be made such that photons cannot enter the calorimeter at angles smaller than a certain value.

The information obtained from this test program will also be very valuable to verify and either prove or disprove another effect predicted by the Monte Carlo simulations. According to GEANT4, the improvement in the em energy resolution achieved by using the signals from *all* fibers is larger than one would (naively) expect to be possible. This is especially true at high energy and for lead as absorber material. Figure 13 shows the simulated response functions for

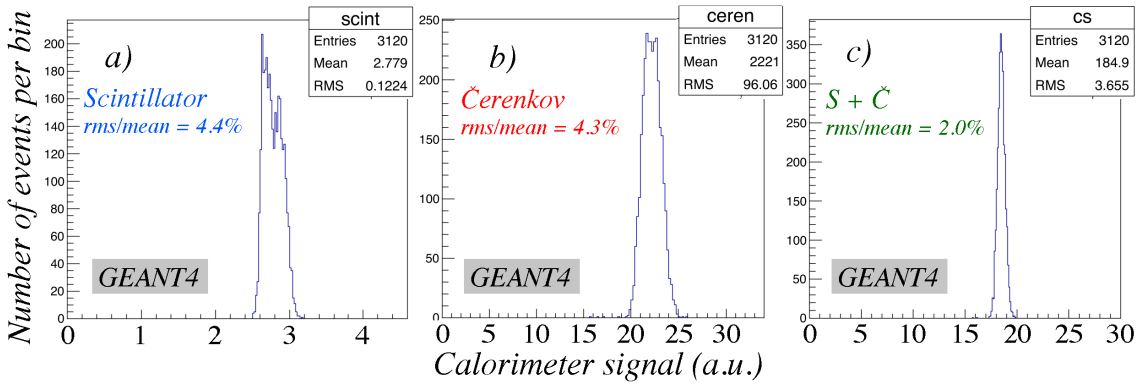

Figure 13: The simulated response functions for 100 GeV electrons in the scintillation (a) and Čerenkov (b) channels, as well as the combined signal distribution (c), in the lead calorimeter. The electrons entered the detector at an angle (1.5°,1.0°).

100 GeV electrons in lead, for the standard angle of incidence (1.5°,1°) used in our previous tests. By combining the signals from the scintillating and the Čerenkov fibers, the resolution improves by more than a factor of two, according to the simulations. Careful investigation has revealed that this phenomenon is caused by a perceived anti-correlation between the scintillation and the Čerenkov signals. This anti-correlation is shown in Figure 14.

At small angles of incidence, the scintillation signal from an electron entering the calorimeter in a scintillating fiber is larger than that from an electron entering the calorimeter in between two scintillating fibers. This difference is due to the (in)efficient sampling of the early, highly

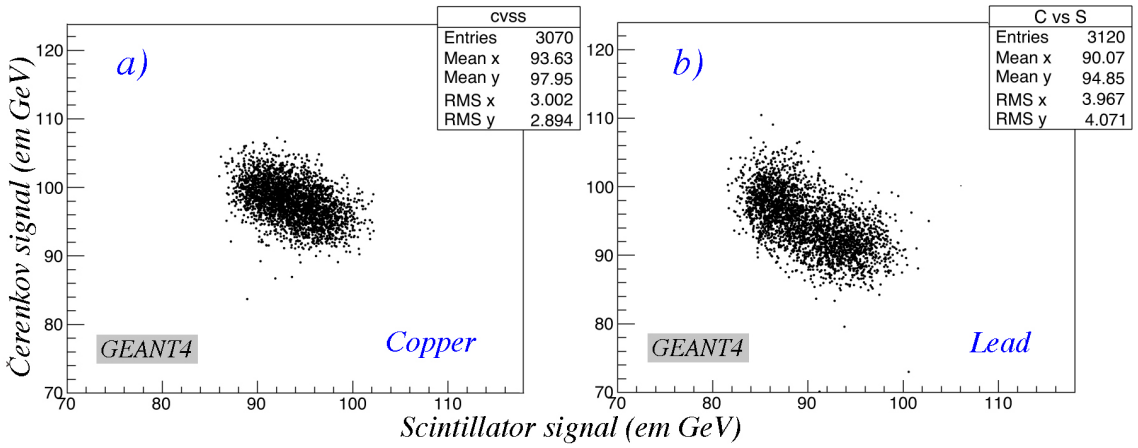

Figure 14: Scatter plot of the Čerenkov versus the scintillation signals for 100 GeV electrons in the copper (a) and lead (b) calorimeter structures. Results from GEANT4 Monte Carlo simulations.

collimated shower component. The anti-correlation shown in Figure 14 implies that a similar effect plays a role for the Čerenkov signals. In that case, a large signal for one fiber type would correspond to a small signal for the other type, and vice versa. However, as discussed in subsection 3.1 and as indicated by the fact that the measured energy resolution scales almost perfectly with $1/\sqrt{E}$ for the Čerenkov signals (see fig. 5), we have no experimental evidence supporting this simulation result. Detailed measurements of the (anti-)correlation between the two types of signals, especially at high energy and at small angles in lead, should shed light on this issue.

There are several other experimental studies we would like to include in our 2014 test beam campaign, time permitting.

- There are other experimental indications that the simulation of the Čerenkov signals leaves something to be desired. For example, we found simulation results for the muon signals that were clearly at variance with the measured reality. The difference between the simulated scintillation and Čerenkov signals for muons was significantly smaller than measured, while the simulated Čerenkov signals were systematically too large (Figure15). It is quite possible that at least some of these discrepancies are the result of a mistreatment of the requirement that the Čerenkov light has to be trapped within the numerical aperture of the fibers in order to contribute to the signals. Until now, the only experimental muon results have come from the original DREAM calorimeter. We are planning to supplement these with some muon measurements in the available RD52 fiber calorimeters.

- Another experimental study we would like to carry out during the test beam period allocated to us in 2014 concerns the possible beneficial effects of increasing the Čerenkov light yield. There are now PMTs available with a photocathode quantum efficiency that is about a factor of two larger than that of our standard PMTs. We will purchase some of these new devices and compare the em resolutions obtained for the Čerenkov channel and for the sum of the scintillation and Čerenkov signals with the values measured with the standard PMTs. This will make it possible to verify simulation predictions of the type

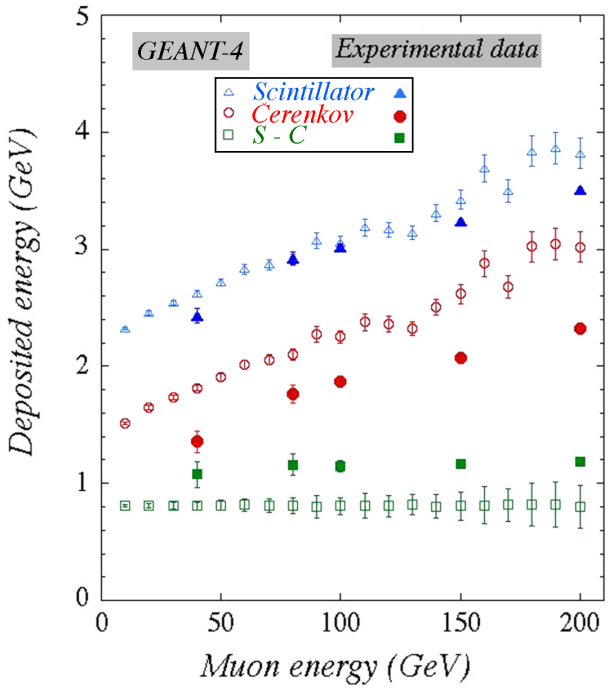

Figure 15: The average energy deposited by muons in the DREAM copper calorimeter, as a function of the muon energy. The experimentally measured results are compared with the GEANT4 simulated ones. The DREAM calorimeter was calibrated with 40 GeV electrons.

shown in Figure 9. These studies should be carried out in a regime where the resolution is dominated by the Čerenkov light yield, *i.e.* with copper absorber, relatively low energy (10 - 20 GeV) and angles that are not close to zero.

- In the same spirit, we would like to do a detailed measurement of the effects of aluminizing the front end of the Čerenkov fibers. One of our copper modules is equipped with such fibers. The inclusion of reflected light in the signals would increase the light yield, and thus improve the em energy resolution. It would also affect the time structure of the signals. The broadening would be larger for hadronic signals than for em ones and, therefore, it would further improve the electron identification probability. The reflected signal is also a measure of the depth at which the generated light is produced, and can thus be used to correct for light attenuation effects. We would like to study these issues experimentally during the 2014 beam tests.

- In a related study, we would like to measure the backward production of Čerenkov light. Until now, we have only measured the Čerenkov/scintillation signal ratios for angles of incidence between 0 and 90°. For technical reasons, it was not possible to go to larger angles. By rearranging the setup on our platform, we want to make it possible to extend the range of these measurements to the backward hemisphere. The results of this study will reveal how much light could potentially be gained from aluminizing the upstream fiber ends.

- Finally, we plan detailed measurements of the time structure of the signals in the leakage counters that surround the fiber calorimeter. When hadrons are sent into the fiber calorimeter, the lateral leakage signal consists of two components: charged particles produced at large angles in the shower development and neutrons that scatter off the protons in the plastic. The latter are of special interest to us, since they allow for additional, independent ways to improve the hadronic resolution ("triple readout" [17]). We hope that the time structure of the signals from the leakage counters will make it possible to distinguish these two components.

4.2 Plans for the longer-term future

Plans for 2015 and beyond include the following:

- Development of absorber structures with considerably higher density. This would make it possible to construct more compact calorimeters of this type. Even though the cost of these new structures is likely to be much higher, this may lead to important overall savings. For example, a 10 m long barrel calorimeter with an inner radius of 1 m would encompass an instrumented volume of about 350 m^3. This could be reduced to 180 m^3 if tungsten were used as absorber material instead of copper.

- Studies of projective calorimeter structures based on the DREAM concept. If a calorimeter of the SuperDREAM type was chosen for a 4π experiment, a projective geometry would be required. This poses a number of complications, which are however not unsolvable. In the context of the RD1 and RD25 projects, fully projective fiber calorimeters have been built [18, 19]. We plan to build on the expertise developed in that context.

- Development of an alternative readout system. Splitting the thousands of fibers sticking out of the back, separating them into scintillating and Čerenkov ones and bunching them accordingly is very cumbersome. Moreover, this system takes up valuable space (≈ 50 cm in the detectors we have built so far), and the fiber bunches may sometimes act as antennas, picking up signals that have nothing to do with the ones for which they are intended. For this reason, we have started to look into a readout system based on silicon photomultipliers. The fibers would no longer stick out of the back, but each fiber would be connected to its own individual SiPM, located at the end face of the absorber structure. Given the large surface area that would have to be covered, such a system is at present still prohibitively expensive. However, given the rapid development of this technology, this might change in the years to come. We are in any case planning to test this idea on a modest scale.

These and other long-term plans depend crucially on a number of issues beyond our control. The most important one is the funding situation. Whereas the funding of the US groups is adequate for the next two years, our Italian collaborators are faced with the fact that INFN no longer supports generic R&D projects such as RD52. This might change if the dual-readout technique were pursued in the context of the development of detectors for new (or upgraded) experiments. In this context, we would like to mention that there are several possibilities in this respect:

- A calorimeter system inspired by DREAM/RD52 is one of the candidates for replacement of the forward calorimeter system of the CMS experiment.
- A cosmic ray experiment to be installed at the future Chinese Space Station has expressed interest in the dual-readout technique, especially because of the electron/hadron separation possibilities and the relative good hadronic performance of a limited-mass calorimeter of this type [20].
- Physicists at the Jefferson Laboratory (US DoE) are interested in a high-precision very forward hadronic calorimeter at an electron-ion collider for forward neutron detection, similar to the H1 use of SPACAL at HERA.

We believe that a dual-readout calorimeter system should also be very seriously considered for an experiment at a future linear electron-positron collider, should such a project become a reality. In that spirit, we aim to perform some dedicated tests that are of interest to the linear collider community when we get an opportunity to test our instruments with hadrons in the H8 beam:

- Measurements of multi-hadron "jets" at 80 and 90 GeV, which should provide an answer to the question how well hadronically decaying W and Z bosons could be distinguished in this device.
- Measurements of the time structure of the signals in neighboring towers for particles entering the detector at an angle θ with the fibers, and determine with what precision the value of this angle could be measured in this longitudinally unsegmented calorimeter.

As explained in Section 4.1, we would need a test beam period of at least two weeks in order to properly assess the hadronic performance of our fiber calorimeter. During such tests, it is also important that we have full control over the polarity and energy of the particles sent from T4 into the H8 beam line. We would, therefore, like to ask the SPS coordinator to keep this in mind when making the 2015 schedule for the H6 and H8 beam lines.

References

[1] DREAM Collaboration (Wigmans R) 2010, CERN-SPSC-2010-012/SPSC-M-771.

[2] DREAM Collaboration (Wigmans R) 2013, CERN-SPSC-2013-012; SPSC-SR-117.

[3] Wigmans R, 2013, *New Results from the RD52 (DREAM) Project*, Nucl. Instr. and Meth. in Phys. Res. **A718** (2013) 43 - 47.

[4] Akchurin N *et al.* 2014, *Particle identification in the longitudinally unsegmented RD52 calorimeter*, Nucl. Instr. and Meth. in Phys. Res. **A735** (2014) 120 - 129.

[5] Akchurin N *et al.* 2014, *The electromagnetic performance of the RD52 fiber calorimeter*, Nucl. Instr. and Meth. in Phys. Res. **A735** (2014) 130 - 144.

[6] Wigmans R 2013, *The dual-readout approach to calorimetry*, Nucl. Instr. and Meth. in Phys. Res. **A732** (2013) 475 - 479.

[7] Akchurin N *et al.* 2014, *Lessons from Monte Carlo simulations of the performance of a dual-readout fiber calorimeter*, submitted to Nucl. Instr. and Meth. in Phys. Res. .

[8] Akchurin N *et al.* 2005, Nucl. Instr. and Meth. in Phys. Res. **A537**, 537.

[9] Groom DE, Nucl. Instr. and Meth. in Phys. Res. **A572** (2007) 633; **A697** (2013) 84; **A705** (2013) 24.

[10] Wigmans R 2008, New Journal of Physics **10**, 025003.

[11] D. Acosta *et al.*, Nucl. Instr. and Meth. in Phys. Res. **A302** (1991) 36.

[12] CALICE Collaboration 2005, CERN-SPSC-2005-036/SPSC-P-328.

[13] Wigmans R 2000, *Calorimetry, Energy Measurement in Particle Physics*, International Series of Monographs on Physics, Vol. 107, Oxford University Press.

[14] Akchurin N *et al.* 2005, Nucl. Instr. and Meth. in Phys. Res. **A536**, 29.

[15] Acosta D *et al.* 1991, Nucl. Instr. and Meth. in Phys. Res. **A308**, 481.

[16] DREAM Collaboration (Wigmans R) 2012, CERN-SPSC-2012-014; SPSC-SR-100.

[17] Akchurin N *et al.* 2009, Nucl. Instr. and Meth. in Phys. Res. **A598**, 422.

[18] Badier J *et al.* 1994, Nucl. Instr. and Meth. in Phys. Res. **A337**, 326.

[19] Anzivino G *et al.* 1995, Nucl. Instr. and Meth. in Phys. Res. **A357**, 350.

[20] Nagaslaev V *et al.* 2001, Nucl. Instr. and Meth. in Phys. Res. **A462** 411.